Received: 1 December 2016 | Accepted: 10 February 2017

DOI: 10.1111/jpi.12399

ORIGINAL ARTICLE

WILEY Journal of Pineal Research
Molecular, Biological, Physiological and Clinical Aspects of Melatonin

Melatonin prevents obesity through modulation of gut microbiota in mice

Pengfei Xu[1] | **Jialin Wang**[1] | **Fan Hong**[1] | **Sheng Wang**[1] | **Xi Jin**[1,2] | **Tingting Xue**[1] | **Li Jia**[1] | **Yonggong Zhai**[1,2]

[1]Beijing Key Laboratory of Gene Resource and Molecular Development, College of Life Sciences, Beijing Normal University, Beijing, China

[2]Key Laboratory for Cell Proliferation and Regulation Biology of State Education Ministry, College of Life Sciences, Beijing Normal University, Beijing, China

Correspondence
Yonggong Zhai, College of Life Sciences, Beijing Normal University, Beijing, China.
Email: ygzhai@bnu.edu.cn

Funding information
National Natural Science Foundation of China, Grant/Award Number: 31571164 and 31271207

Abstract

Excess weight and obesity are severe public health threats worldwide. Recent evidence demonstrates that gut microbiota dysbiosis contributes to obesity and its comorbidities. The body weight-reducing and energy balancing effects of melatonin have been reported in several studies, but to date, no investigations toward examining whether the beneficial effects of melatonin are associated with gut microbiota have been carried out. In this study, we show that melatonin reduces body weight, liver steatosis, and low-grade inflammation as well as improving insulin resistance in high fat diet (HFD)-fed mice. High-throughput pyrosequencing of the 16S rRNA demonstrated that melatonin treatment significantly changed the composition of the gut microbiota in mice fed an HFD. The richness and diversity of gut microbiota were notably decreased by melatonin. HFD feeding altered 69 operational taxonomic units (OTUs) compare with a normal chow diet (NCD) group, and melatonin supplementation reversed 14 OTUs to the same configuration than those present in the NCD group, thereby impacting various functions, in particular through its ability to decrease the *Firmicutes*-to-*Bacteroidetes* ratio and increase the abundance of mucin-degrading bacteria *Akkermansia*, which is associated with healthy mucosa. Taken together, our results suggest that melatonin may be used as a probiotic agent to reverse HFD-induced gut microbiota dysbiosis and help us to gain a better understanding of the mechanisms governing the various melatonin beneficial effects.

KEYWORDS

gut microbiota, inflammation, insulin resistance, liver steatosis, melatonin, obesity

1 | INTRODUCTION

Excess weight and obesity, characterized by a high body mass index (BMI), have doubled worldwide since the 1980s, according to the 2014 Global Status Report from the World Health Organization.[1] Globally, about 2 billion adults were overweight (BMI≥25 kg/m^2) and more than 600 million were obese (BMI≥30 kg/m^2) in 2014, while 42 million children (<5 years old) were overweight, or obese in 2013.[1] The obesity prevalence is increasing everywhere. In the United States, which is considered as one of the countries with the highest prevalence of obesity, about 70% of adults are considered overweight, including 36% obese individuals.[2,3] China has a lower rate (5.2%, in 2010) of obesity, but the absolute number of obese people exceeds that of the United States.[2,4] To date, numerous studies have reported that excess body weight is a known risk factor associated with mortality from cancer and some other chronic diseases, including diabetes, fatty liver disease, and cardiovascular diseases.[5,6] Obesity has been surpassing tobacco smoking and has become the most important global public health concern today.[7,8]

© 2017 John Wiley & Sons A/S. Published by John Wiley & Sons Ltd

Increasing evidence indicates that the changes in gut microbiota composition are associated with obesity and its associated metabolic disorders.[9] Moreover, genetic- and dietary-induced obese rodents showed large increases in their *Firmicutes*/*Bacteroidetes* ratio.[10,11] Transplanting the gut microbiota isolated from high fat diet (HFD)-induced obese donors to germ-free animals led to a significant increase in body weight and metabolic syndrome in the recipient mice.[12] The positive effect of gut microbiota on energy metabolism and nutrient acquisition may have the potential to prevent obesity.

Melatonin, or N-acetyl-5-methoxy tryptamine, is a natural molecule widely present in animals, plants, bacteria, fungi, and eukaryotic protists.[13-17] In mammals, including humans, pineal melatonin is a natural hormone secreted from the pineal gland situated in the brain. It plays a key role in the regulation of other hormones and maintains the circadian rhythm. Several studies showed that circadian rhythm melatonin is involved in the regulation of body weight gain and energy metabolism in some rodents.[18-22] Moreover, in Zucker diabetic fatty rats,melatonin has been proved to ameliorate low-grade inflammation and oxidative stress,[23] improve glucose homeostasis and dyslipidemia,[24] stimulate browning of inguinal subcutaneous adipose tissue (Ing-SAT),[25] and reduce mitochondrial dysfunction in liver, skeletal muscle, and Ing-SAT.[26-28] However, there are no clinical or experimental studies that evaluated the effects of melatonin on the gut microbial dysbiosis induced by HFD. Therefore, whether melatonin, as a probiotic, prevents obesity by modulating the gut microbiota is still unknown. In this study, we observed that melatonin prevents HFD-induced obesity, liver steatosis, insulin resistance, and low-grade inflammation. Through the gut microbiota profiling, our results indicate that melatonin induces a substantial change in gut microbiota composition, suggesting a potential mechanism by which melatonin reduces obesity and its related disorders.

2 | MATERIALS AND METHODS

2.1 | Drug and diets

Melatonin (M5250) was purchased from Sigma-Aldrich (St Louis, MO, USA). Both the normal chow diet (NCD) and HFD (containing 60% kcal fat) were purchased from Beijing HFK Bioscience Co. Ltd., (Beijing, China).

2.2 | Animals and experimental design

Ten-week-old male C57BL/6J mice were obtained from Vital River Laboratory Animal Technology Co. Ltd (Beijing, China). After a 1 week adaptation period, the mice were randomly assigned to three groups (n=6-15) in a light and climate controlled room at 12-hours light—12-hours dark cycle and 25±2°C, with free access to water and different diets. The melatonin treatment group (HFD+M) was fed an HFD with melatonin at 50 mg/kg body weight (BW) by gavage once daily for 10 weeks. All experimental procedures were performed and approved by the guidelines of Ethics and Animal Welfare Committee of Beijing Normal University. (Approval No. CLS-EAW-2015-013). All efforts were made to reduce animal suffering.

2.3 | Histological analysis

To make paraffin section, epididymal white adipose tissue (Epi-WAT) and brown adipose tissue (BAT) were fixed in 4% paraformaldehyde, paraffin-embedded and sectioned at 5-7 μm. Hematoxylin and eosin (H&E) staining was according to standard method. The size of adipocytes from Epi-WAT was analyzed using a Cell Profiler Software, as previously.[29] For immunofluorescence, briefly, BAT sections were incubated with UCP1 (Sigma), diluted at 1:100, at 4°C for 12 hours, and then incubated with the secondary antibody for 1 hour. Liver frozen sections (8-10 μm) were stained with Oil Red O.

2.4 | Biochemical analysis

Blood samples were collected from fasted mice at the end of the experiment. Serum total cholesterol (TC), triacylglycerol (TG), as well as glucose, and liver TG concentrations were measured using commercially available kits from Beijing Applygen Technologies Inc. (Beijing, China). Serum levels of insulin, tumor necrosis factor-α (TNF-α), and interleukin-6 (IL-6) were detected using commercially available ELISA kits from Neobioscience Technology Company (Shenzhen, China). Serum LPS concentration was measured using a quantitative chromogenic tachypleus amebocyte lysate kit from Chinese Horseshoe Crab Reagent Manufactory, Co., Ltd (Xiamen, China).

2.5 | Glucose and insulin tolerance analyses

For the intraperitoneal glucose tolerance test (IPGTT), during the 8th week of the experiment, mice were fasted for 12 hours before receiving an intraperitoneal injection of D-glucose (1.5 g/kg). Blood samples were taken from the tail vein at different time points, and blood glucose was measured using a glucometer (Johnson & Johnson, Shanghai, China). For the insulin tolerance test (ITT), during the 9th week of the experiment, mice were fasted for 6 hours before receiving an intraperitoneal injection of insulin (0.75 UI/kg; Novo Nordisk). Blood samples were taken, and blood glucose levels were measured. Using serum fasting blood glucose and insulin concentrations, we calculated the homeostasis model index of insulin resistance (HOMA-IR: insulin×glucose/22.5) and

the quantitative insulin check index of insulin sensitivity (QUICKI: 1/[log (insulin)+log (glucose)]) as previously.[30]

2.6 | Western blot analysis

Liver protein was extracted using RIPA lysis. The protein amount was measured using a BCA protein assay reagent from Pierce (Rockford, IL, USA). Protein samples were separated by 10% SDS-PAGE gel and transferred onto Immobilon®-P transfer membranes. After blocking with 8% nonfat milk, membranes were first incubated with primary antibodies, against FAS (1:2000), NF-κB (1:2000), IκB-α (1:1000), and β-actin (1:6000) at 4°C for 12 hours, and then with the secondary antibody for 1 hour, as described previously.[31] The intensities of protein bands were quantified with the ImageJ software and the values normalized to β-actin.

2.7 | Gene expression analysis

Tissue total RNA was isolated with an RNAprep Pure tissue kit from Tiangen Biotech Co., Ltd. (Beijing, China). For real-time PCR analysis, reverse transcription was performed with oligdT-18 and M-MLV transcriptase from Promega (Madison, WI, USA). SYBR Green qPCR SuperMix was performed on an ABI 7500 real-time PCR system according to the manufacturer's instructions, as we described previously.[31] Values were normalized against control glyceraldehyde-3-phosphate dehydrogenase (GAPDH). Sequences of the real-time PCR primers used are listed in Table S1.

2.8 | Gut microbiota analysis

Fresh fecal samples were collected during the final 5 days for the gut microbial analysis. Bacterial genomic DNA was extracted from frozen fecal samples stored at −80°C using QIAamp DNA stool Mini Kit from Qiagen (Hilden, Germany), according to the manufacturer's instructions. The 16S rRNA gene comprising V3 and V4 regions was amplified by PCR using composite specific bacterial primers (Table S1). Thermal cycling consisted of the following condition: 95°C for 5 minutes (1 cycle), 95°C for 30 s/50°C for 30 s/72°C for 40 seconds (25cycles), and a final extension at 72°C for 7 minutes. High-throughput pyrosequencing of the PCR products was performed on an Illumina MiSeq platform at Biomarker Technologies Co, Ltd. (Beijing, China).

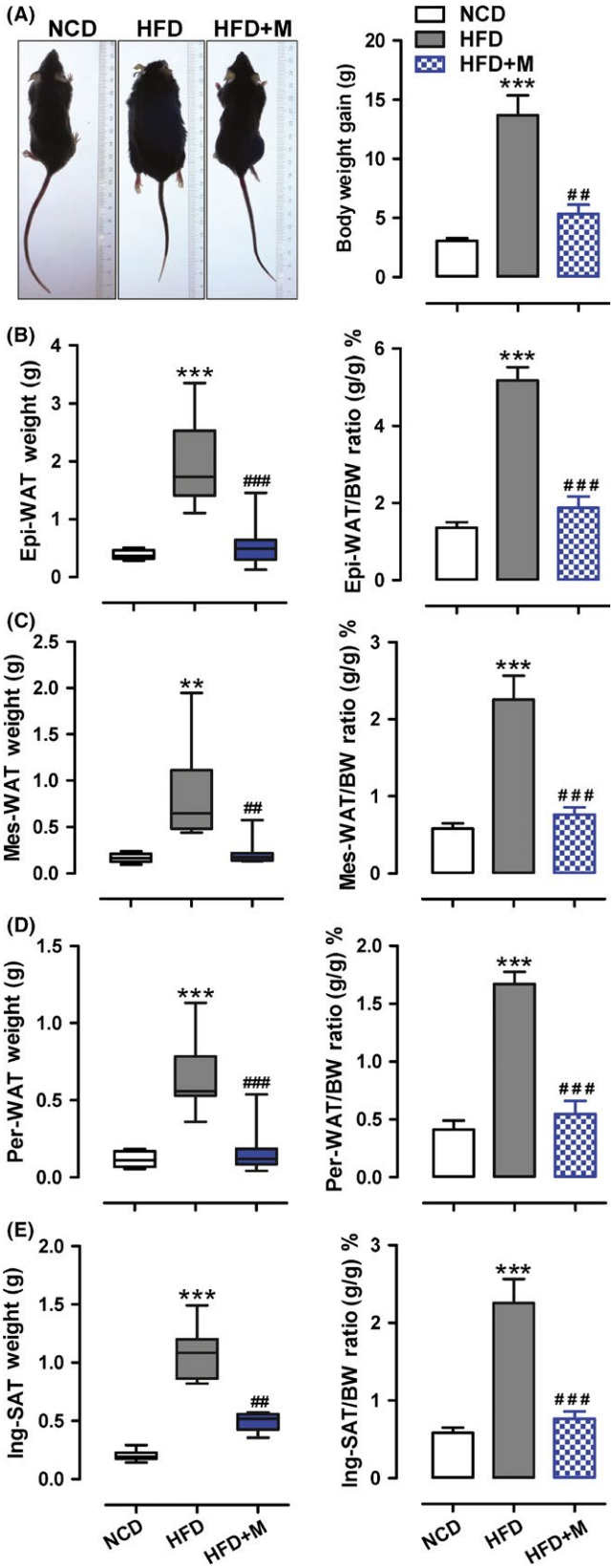

FIGURE 1 Effects of melatonin on body weight gain in high fat diet (HFD)-fed mice. (A) Representative mice and body weight gain, (B) epididymal white adipose tissue (Epi-WAT) weight and Epi-WAT/BW ratio, (C) mesenteric white adipose tissue (Mes-WAT) weight and Mes-WAT/BW ratio, (D) perirenal white adipose tissue (Per-WAT) weight and Per-WAT/BW ratio, and (E) inguinal subcutaneous adipose tissue (Ing-SAT) weight and Ing-SAT/BW ratio in male C57BL/6J mice fed a normal chow diet (NCD, n=6), HFD, n=10), or HFD with melatonin (HFD+M, n=15) gavage (50 mg/kg/d) for 10 wk. Values are presented as mean±SE. Differences were assessed by ANOVA and denoted as follows: $^{**}P<.01$; $^{***}P<.001$ compared with NCD, $^{\#\#}P<.01$; $^{\#\#\#}P<.001$ compared with HFD

The raw paired-end reads from the original DNA fragments were merged using FLASH[32] and assigned to each sample according to the unique barcodes. High-quality reads for bioinformatics analysis were performed, and all of the effective reads from each sample were clustered into operational taxonomic units (OTUs) based on a 97% sequence similarity according to UCLUST.[33] For alpha diversity analysis, we rarified the OTU to several metrics, including curves of OTU rank, rarefaction and Shannon, and calculated indexes of Shannon, Chao1, Simpson, and ACE. For beta-diversity analysis, heatmap of RDA-identified key OTUs, principal component analysis (PCA), principal coordinate analysis (PCoA), nonmetric multidimensional scaling (NMDS), and unweighted pair group method with arithmetic mean (UPGMA) were performed using QIIME.[34] The LDA effect size (LEfSe) analysis was performed for the quantitative analysis of biomarkers among each group.[35] Briefly, LEfSe analysis, LDA threshold of>4, used the nonparametric factorial Kruskal-Wallis (KW) sum-rank test and then used the (unpaired) Wilcoxon rank-sum test to identify the most differently abundant taxa.

2.9 | Statistical analysis

Results were presented as means±SE. The statistical analysis was performed using SPSS, version 20 (IBM, Armonk,

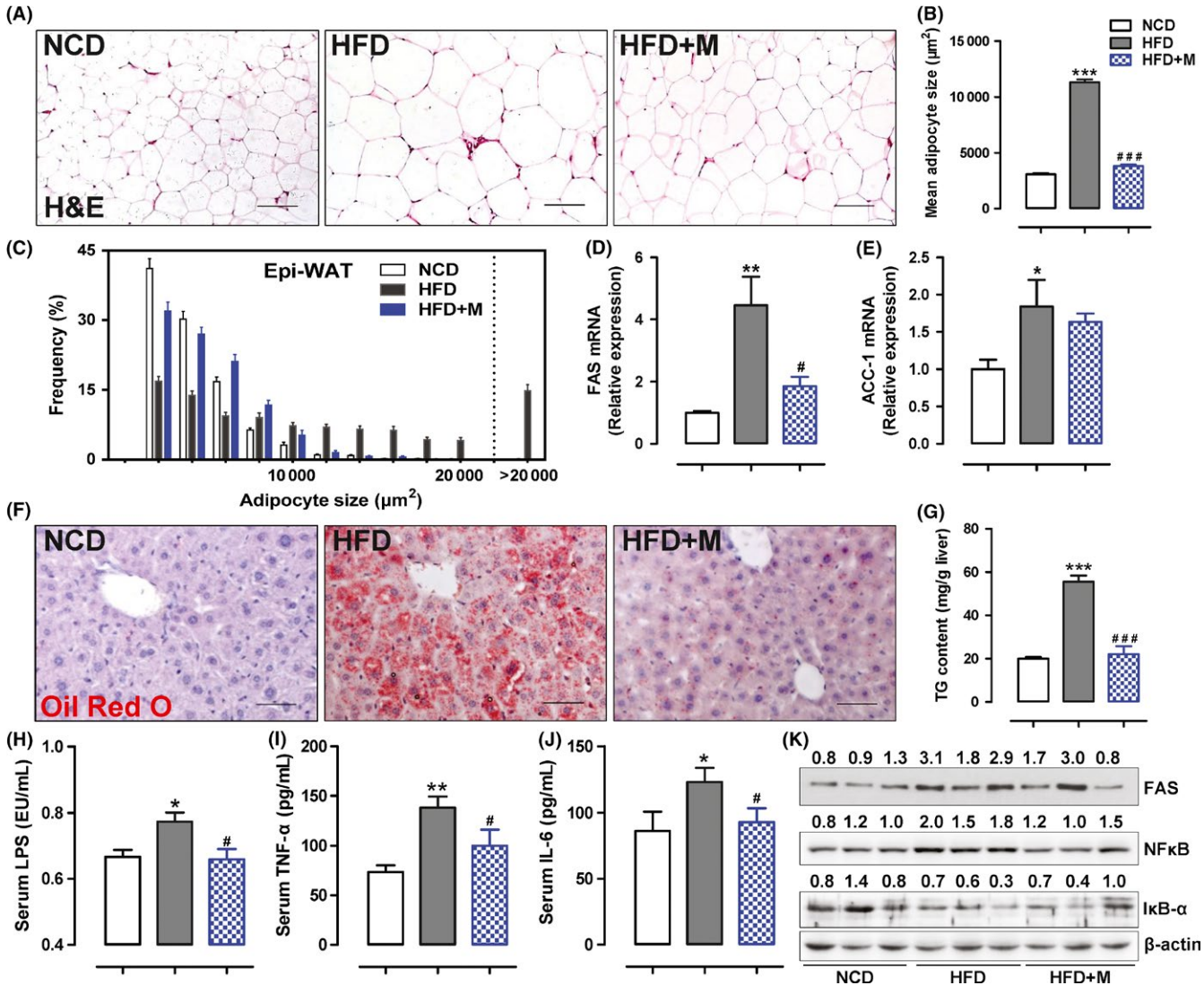

FIGURE 2 Effects of melatonin on adipocyte hypertrophy, hepatic steatosis, and systemic inflammation in high fat diet (HFD)-fed mice. (A) H&E staining of epididymal white adipose tissue (Epi-WAT) sections (scale: 100 μm). (B) Mean adipocyte size and (C) epididymal adipocyte size distribution in each group (n=5, 20 microscopic images were obtained from each treatment group). (D and E) Epi-WAT mRNA expression of genes involved in lipogenesis was measured by real-time PCR analysis. Liver Oil Red O staining (F) and triacylglycerol (TG) concentrations (G) were analyzed at the end of the study (scale: 50 μm). (H) Serum endotoxin was determined using the limulus amebocyte lysate assay kit. Serum tumor necrosis factor-α (TNF)-α (I) and IL-6 (J) concentrations were measured by ELISA. Values are means±SE. (K). The liver FAS, NFκB, and IκB-α protein production was examined by Western blotting, and relative protein levels were normalized with β-actin (n=3). Differences were assessed by ANOVA and denoted as follows: $^{*}P<.05$; $^{**}P<.01$; $^{***}P<.001$ compared with normal chow diet (NCD), $^{\#}P<.05$; $^{\#\#\#}P<.001$ compared with HFD

NY, USA). Differences between groups were statistically analyzed using ANOVA followed by Tukey's multiple comparison tests and unpaired *t* tests and considered statistically with a level of $P<.05$.

3 | RESULTS

3.1 | Melatonin reduces body weight gain in HFD-fed mice

To determine the effect of melatonin on body weight gain under HFD, 10-week-old male C57BL/6J mice were fed either a NCD or HFD for 10 weeks and were supplemented with melatonin simultaneously (50 mg/kg/d) by gavage. As expected, HFD mice gained more weight compared to the NCD mice. Supplementation with melatonin significantly prevented the body weight gain in HFD-fed mice (Figure 1A). We then isolated the four main types of adipose tissues from the mice: Epi-WAT, mesenteric white adipose tissue (Mes-WAT), perirenal white adipose tissue (Per-WAT), and Ing-SAT. As shown in Figure 1B-E, consistent with the body weight gain, all four types of adipose tissues weights and the ratio of various adipose tissues normalized to body weights were obviously increased by HFD ($P<.001$) and decreased by melatonin supplementation ($P<.001$) in mice.

3.2 | Melatonin prevents HFD-induced WAT hypertrophy, liver steatosis and systemic low-grade inflammation

Next, we examined the size of adipocyte cells obtained from Epi-WAT sections (Figure 2A). The adipocyte size was measured using automated image analysis. As shown in Figure 2B,C, the HFD group exhibited a larger mean adipocyte size compared to the NCD group, while this size was kept at a normal level in the HFD+M group, reflecting the decreased frequency of larger adipocytes (>12 000 μm^2) and the increased frequency of smaller adipocytes (2000-8000 μm^2). We measured the expression of lipogenic genes, including FAS and ACC-1 in the Epi-WAT. As shown in Figure 2D,E, the HFD promoted the expression of lipogenic genes, and melatonin treatment significantly inhibited the FAS gene expression. Significant inhibition of FAS protein expression was also observed in the liver (Figure 2K). The inhibition of lipogenesis was closely correlated with the ameliorated hepatic steatosis. As shown in Figure 2F,G, Oil Red O staining and liver TG content measurements indicated that

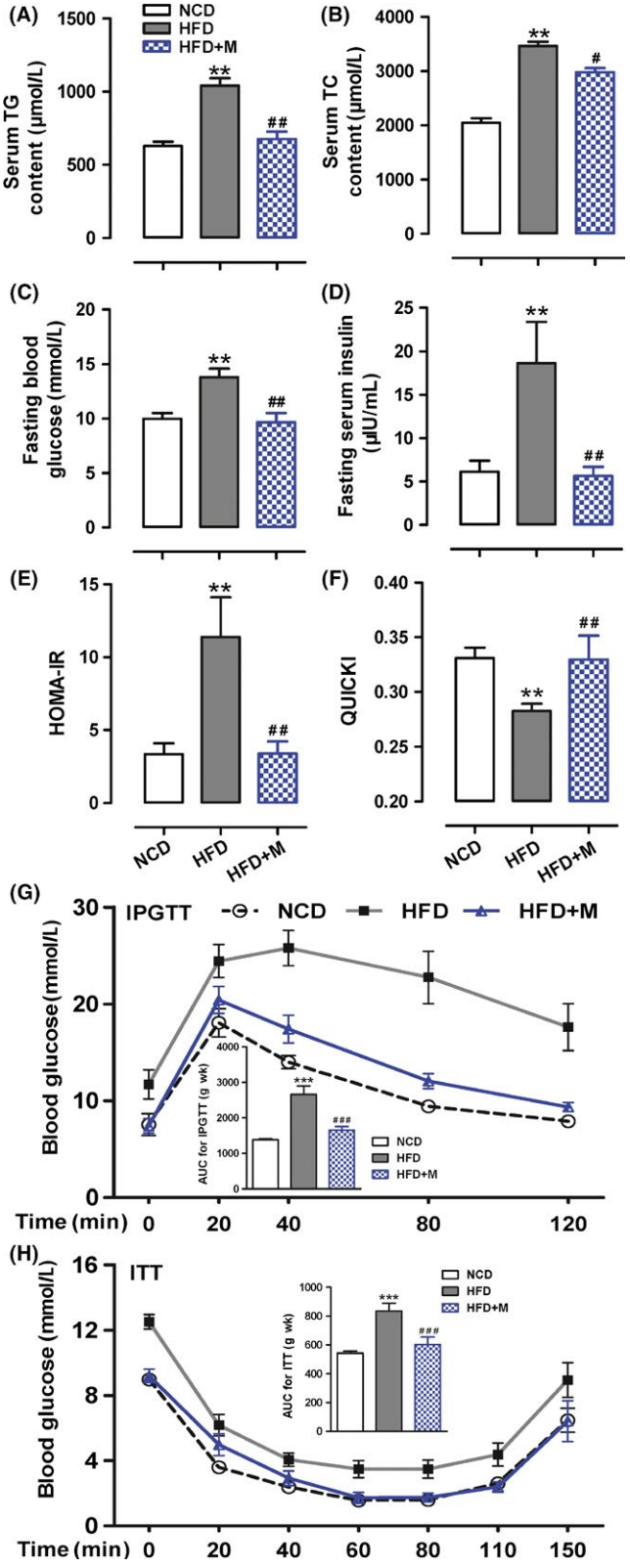

FIGURE 3 Preventive effects of melatonin on the development of insulin resistance in high fat diet (HFD)-fed mice. Serum concentrations of triacylglycerol (TG) (A) and total cholesterol (TC) (B), fasting blood glucose (C), and insulin (D) in the mice shown in Figure 1. (E) HOMA-IR and (F) QUICKI calculated according to the formula. (G) intraperitoneal glucose tolerance test (IPGTT) and (H) insulin tolerance test(ITT) test (n=5). Curves of blood glucose levels and the calculated AUC (inner graph) are shown. Values are expressed as mean±SE. Differences were assessed by ANOVA and denoted as follows: $^{**}P<.01$; $^{***}P<.001$ compared with normal chow diet (NCD), $^{\#}P<.05$; $^{\#\#}P<.01$; $^{\#\#\#}P<.001$ compared with HFD

melatonin markedly inhibited the liver lipid accumulation and prevented liver steatosis in mice fed an HFD. Previous studies have shown that obesity and liver steatosis are associated with low-grade chronic inflammation.[36] We investigated the effects of melatonin on serum endotoxins (that is, LPS) and inflammatory cytokines (TNF-α and IL-6) levels. Melatonin treatment reduced endotoxemia and systemic low-grade inflammation in HFD-fed obese mice (Figure 2H-J). Because NF-κB is a key player in inflammatory reactions, HFD feeding significantly enhanced the production of NF-κB and reduced IκB-α protein expression in the liver, while melatonin supplementation restored their levels (Figure 2K).

3.3 | Melatonin improves HFD-induced glucose tolerance and insulin resistance

To examine the ability of melatonin to attenuate hyperlipidemia, we measured the serum lipid concentration. As shown in Figure 3A,B, after 10 weeks on the experimental diets, the TG and TC concentrations were significantly increased by HFD feeding (+65.6% and +69.1%, respectively) compared to the NCD and were decreased by melatonin treatment −35.1% and −14%, respectively). As obesity is strongly associated with glucose tolerance and insulin resistance, we measured the fasting blood glucose and insulin concentrations and calculated the HOMA-IR and QUICKI according to previously determined formulas. As shown in Figure 3C-F, melatonin administration clearly preserved insulin sensitivity in obese mice and reversed fasting blood glucose and insulin concentrations, and the two calculated indexes, to nearly normal levels. Results of the IPGTT and ITT, and the corresponding area under curve (AUC) values, further confirmed that melatonin supplementation notably ameliorated the impaired glucose tolerance and insulin resistance in HFD-fed mice (Figure 3G,H).

3.4 | Melatonin stimulates BAT browning in HFD-fed mice

Melatonin promotes the growth of BAT in different species.[37,38] As shown in Figure 4A, HFD-fed mice showed enhanced lipid accumulation (that is, "whitening"), and oral administration with melatonin reversed the HFD-induced whitening and increased the protein expression of thermogenic marker uncoupling protein 1 (UCP1) in BAT. Furthermore, in the BAT, the mRNA expression of thermogenic genes (UCP1 and UCP3) was significantly increased (Figure 4B,C), and the mRNA expression levels of mitochondrial biogenesis (PGC1α), fatty acid catabolism (CPT1β), and lipid transport (CD36 and FABP) were also mildly increased in melatonin-treated mice, although these differences were not statistically significant (Figure 4D-G). These results showed that melatonin stimulates BAT browning and thermogenesis in HFD-induced obese mice.

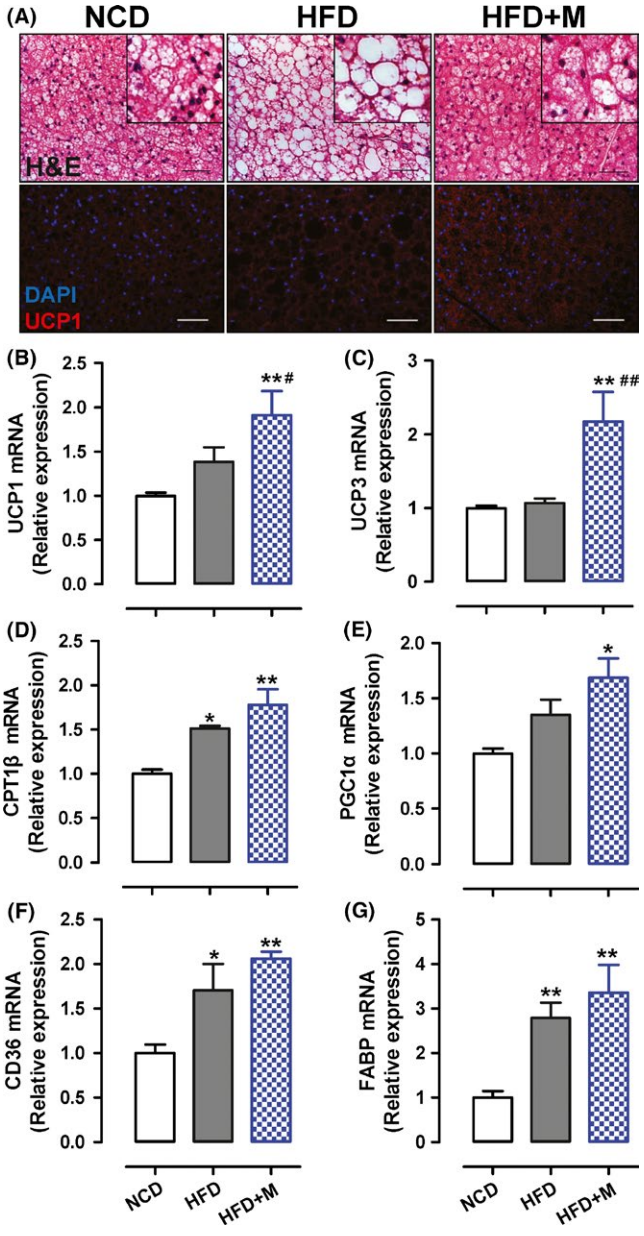

FIGURE 4 Effects of melatonin on brown adipose tissue (BAT) browning in high fat diet (HFD)-fed mice. (A) H&E and uncoupling protein1 (UCP1) immunofluorescence staining of representative BAT sections (scale: 50 μm). (B-G) Relative mRNA expression of markers for thermogenesis (UCP1 and UCP3), mitochondrial biogenesis(PGC1α), fatty acid catabolism (CPT1β), and lipid uptake (CD36 and FABP) in BAT (n=3). Values are presented as mean±SE. Differences were assessed by ANOVA and denoted as follows: $^{*}P<.05$; $^{**}P<.01$ compared with normal chow diet (NCD), $^{\#}P<.05$; $^{\#\#}P<.01$ compared with HFD

3.5 | Melatonin alters the gut microbiota composition in HFD-induced mice

The interaction between HFD feeding and gut microbiota has been suggested to be involved in the above obesity-associated metabolic disorder. We assessed the effects of melatonin on

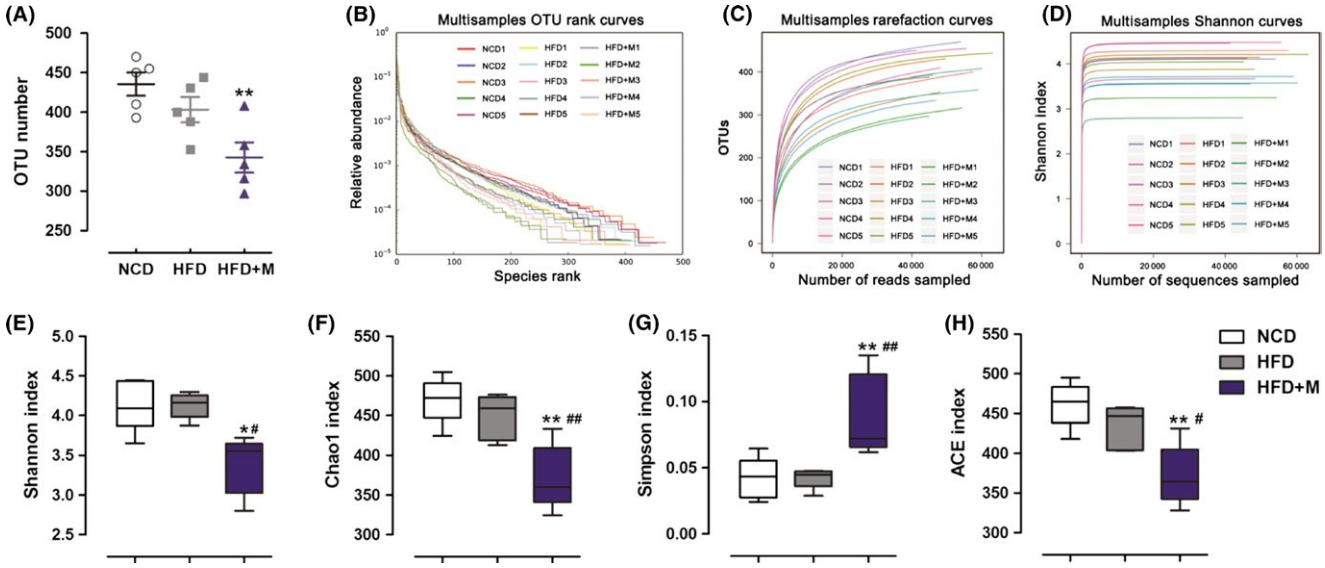

FIGURE 5 Responses of the diversity, richness, and structure of the gut microbiota to melatonin during the treatment of obesity in mice. (A) operational taxonomic units (OTU) number of gut microbiota in three groups; (B-D) OTU rank curves, rarefaction curves and Shannon curves of gut microbiota for each sample, respectively; (E-H) shows the Shannon index, Chao1 index, Simpson index, and ACE index of each group. Values are presented as mean±SE. (n=5). Differences were assessed by ANOVA and denoted as follows: $^{*}P<.05$; $^{**}P<.01$ compared with normal chow diet (NCD), $^{\#}P<.05$; $^{\#\#}P<.01$ compared with high fat diet(HFD). Relative abundances of the gut microbiota at phylum level (I) and genus level (J). (K) Weighted Unifrac cluster tree based on group method with arithmetic mean (UPGMA). (L-N) nonmetric multidimensional scaling (NMDS) score plot based on Bray-Curtis, PCoA score plot, and principal component analysis (PCA) score plot based on weights

the intestinal microbiota composition by sequencing the bacterial 16S rRNA V3+V4 region. High-throughput pyrosequencing of the samples produced 914 756 raw reads. After removing the low-quality sequences, 795 719 clean tags were subjected to the following analysis (Table S2). Based on 97% similarity level, all of the effective reads were clustered into OTUs. As shown in Figure 5A, there was no significant difference in the number of OTUs between HFD and NCD groups, while melatonin decreased the number of OTUs. The curves of OTU rank (Figure 5B), rarefaction (Figure 5C), and Shannon (Figure 5D), as well as the indexes of Shannon (Figure 5E), Chao1 (Figure 5F), Simpson (Figure 5G), and ACE (Figure 5H) were calculated. Consistent with the number of OTUs, melatonin treatment significantly reduced both the richness and diversity of the intestinal microbiota in HFD-fed mice. As shown in Figure 5I, the phylum level analysis demonstrated that HFD feeding significantly decreased the relative abundance of *Bacteroidetes* and increased the relative abundance of *Firmicutes*, while the treatment with melatonin restored these levels and reduced the ratio of *Firmicutes* to *Bacteroidetes*. Interestingly, melatonin supplementation notably increased the abundance of *Verrucomicrobia*. To further exhibit the differences among each sample, the genus level analysis was performed, showing results similar to those observed at the phylum level. As shown in Figure 5J, melatonin treatment significantly increased the relative abundance of *Akkermansia* belonging to the *Verrucomicrobia* phylum in HFD-fed mice. Weighted Unifrac cluster tree based on UPGMA revealed great modulating effects of melatonin on the intestinal microbiota structure (Figure 5K). The intestinal microbiota structural changes were then analyzed using unsupervised multivariate statistical methods including, nonmetric multidimensional scaling (NMDS), UniFrac distance-based principal coordinate analysis (PCoA), and principal component analysis (PCA). As shown in Figure 5L-N, all three groups presented a distinct clustering of microbiota composition, and the HFD+M group had a similar structure to that of the HFD group.

3.6 | Melatonin modulates the key phylotypes of gut microbiota in HFD-fed mice

To identify the gut microbiota phylotypes responding to melatonin supplementation, we analyzed the effective sequences of all samples by redundancy analysis (RDA). As shown in Figure 6A,B and Data S1, a total of 85 predictive OTUs were identified among three groups, and HFD feeding altered 69 OTUs (27 increased and 42 decreased) compare with the NCD group. Treatment with melatonin generated 30 OTUs changes (10 increased and 20 decreased) compare with the HFD group, and among these changes, 14 OTUs were reversed to the same direction than those observed within the NCD group. A detailed analysis of the above 14 OTUs indicated that *Ruminococcaceae,*[39] *Desulfovibrionaceae,*[40] *Bacteroides, Porphyromonadaceae,*[41] *Helicobacteraceae,*[42] and *Christensenellaceae* were all reversed by melatonin, and most of them have been positively correlated with obesity and its related disorders in previous studies.

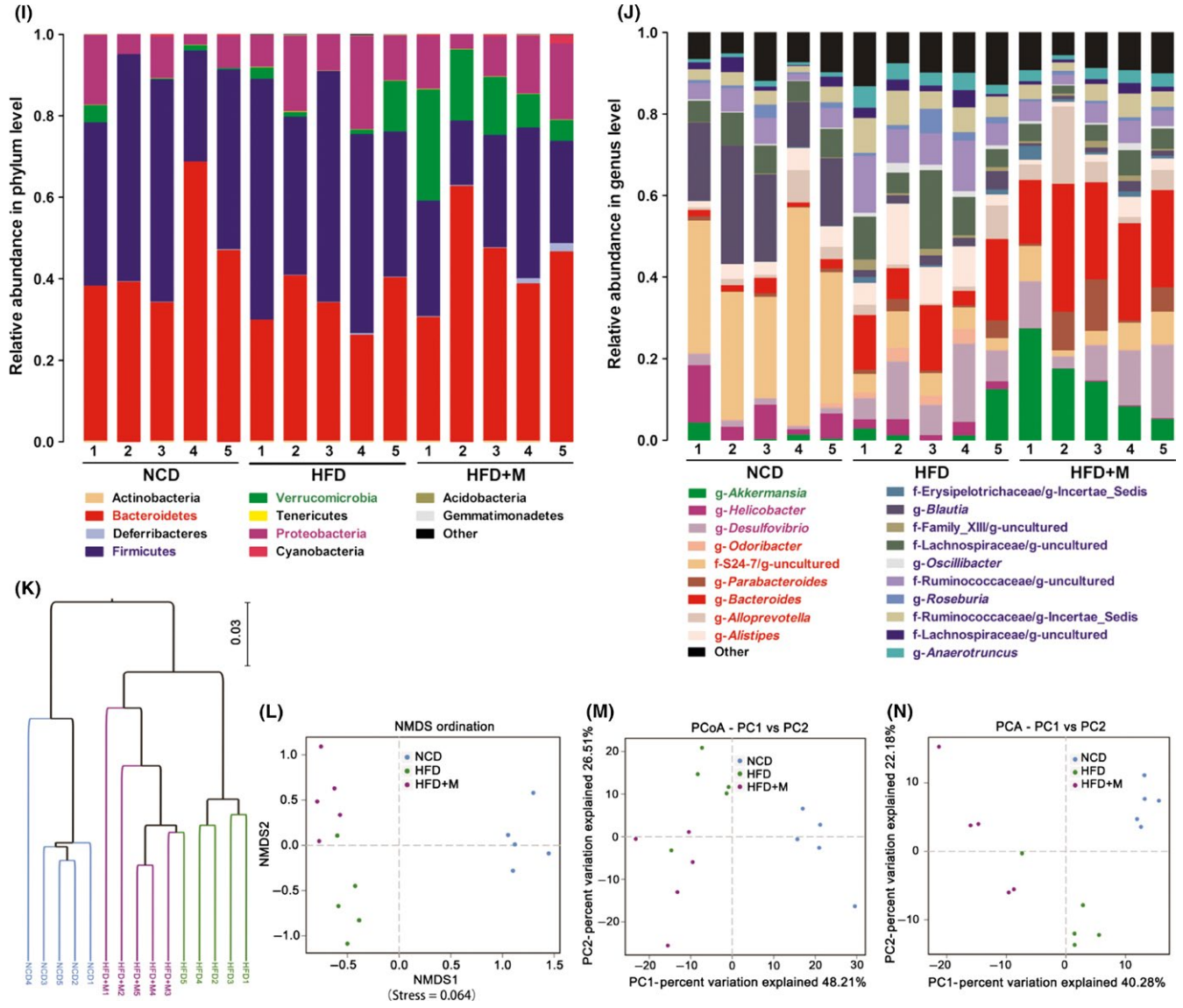

FIGURE 5 (Continued)

LEfSe analysis identified the high-dimensional biomarkers in the intestinal microbiota among each group. As shown in Figure 7A, melatonin supplementation induced a trend of a large increase in *Akkermansia*, which is a probiotic that helps reduce HFD-induced obesity, diabetes, and inflammation. The relative abundance of bacteria, having negative effects, including *Alistipes*, *Anaerotruncus,* and *Helicobacter marmotae* were all reduced after melatonin treatment in HFD-fed mice (Figure 7B-D). Collectively, these results indicate that melatonin treatment reverses HFD-induced gut microbiota dysbiosis.

4 | DISCUSSION

Gut microbiota is closely correlated with obesity. Although several studies have shown that melatonin prevents obesity in different animal models,[18,20,21,43,44] the effects of melatonin on the gut microbiota had not yet been investigated. In this study, we investigated the effects of melatonin oral administration for 10 weeks on the development of obesity and gut microbiota. Our results revealed that melatonin has a protective effect against dietary-induced obesity, insulin resistance, liver steatosis, and low-grade inflammation. Additionally,

FIGURE 6 Heatmap of redundancy analysis (RDA)-identified key operational taxonomic units (OTUs) and LefSe identifies the most differently abundant taxons in gut microbiota in response to melatonin treatment. (A) Heat map showing the relative abundance of RDA-identified key 85 OTUs significantly altered by melatonin in high fat diet (HFD)-fed mice. (B) Represented bacterial taxa information (genus, family, and phylum) of OTUs from (A)is shown. Red arrows and blue arrows indicate the OTUs that increased or decreased in the normal chow diet (NCD) and HFD+M groups relative to the HFD group based on Turkey's HSD test ($P<.01$)

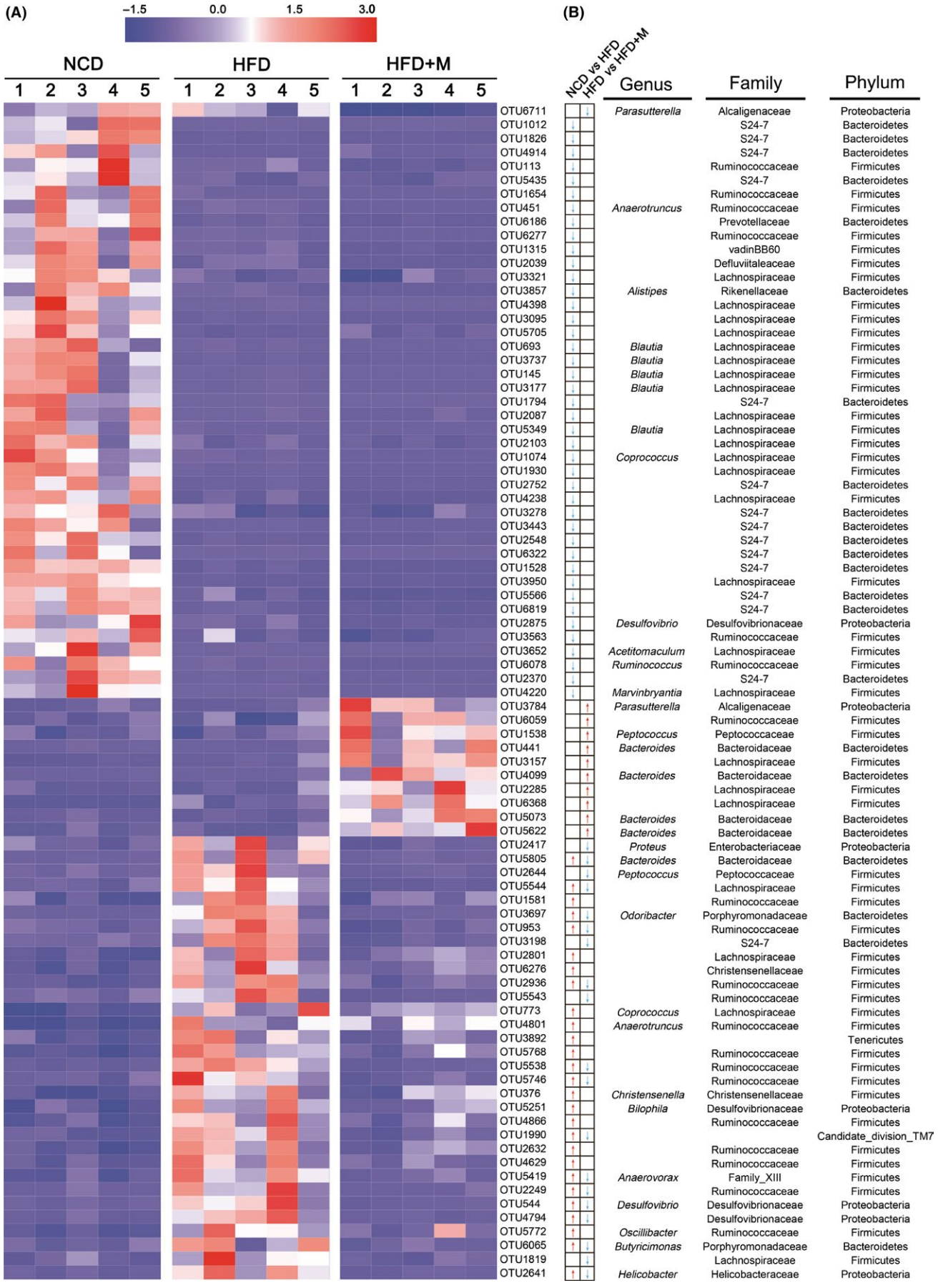
(A)
−1.5
0.0
1.5
3.0
NCD
HFD
HFD+M
1 2 3 4 5
(B)
NCD vs HFD
HFD vs HFD+M
Genus
Family
Phylum
OTU6711 Parasutterella Alcaligenaceae Proteobacteria
OTU1012 S24-7 Bacteroidetes
OTU1826 S24-7 Bacteroidetes
OTU4914 S24-7 Bacteroidetes
OTU113 Ruminococcaceae Firmicutes
OTU5435 S24-7 Bacteroidetes
OTU1654 Ruminococcaceae Firmicutes
OTU451 Anaerotruncus Ruminococcaceae Firmicutes
OTU6186 Prevotellaceae Bacteroidetes
OTU6277 Ruminococcaceae Firmicutes
OTU1315 vadinBB60 Firmicutes
OTU2039 Defluviitaleaceae Firmicutes
OTU3321 Lachnospiraceae Firmicutes
OTU3857 Alistipes Rikenellaceae Bacteroidetes
OTU4398 Lachnospiraceae Firmicutes
OTU3095 Lachnospiraceae Firmicutes
OTU5705 Lachnospiraceae Firmicutes
OTU693 Blautia Lachnospiraceae Firmicutes
OTU3737 Blautia Lachnospiraceae Firmicutes
OTU145 Blautia Lachnospiraceae Firmicutes
OTU3177 Blautia Lachnospiraceae Firmicutes
OTU1794 S24-7 Bacteroidetes
OTU2087 Lachnospiraceae Firmicutes
OTU5349 Blautia Lachnospiraceae Firmicutes
OTU2103 Lachnospiraceae Firmicutes
OTU1074 Coprococcus Lachnospiraceae Firmicutes
OTU1930 Lachnospiraceae Firmicutes
OTU2752 S24-7 Bacteroidetes
OTU4238 Lachnospiraceae Firmicutes
OTU3278 S24-7 Bacteroidetes
OTU3443 S24-7 Bacteroidetes
OTU2548 S24-7 Bacteroidetes
OTU6322 S24-7 Bacteroidetes
OTU1528 S24-7 Bacteroidetes
OTU3950 Lachnospiraceae Firmicutes
OTU5566 S24-7 Bacteroidetes
OTU6819 S24-7 Bacteroidetes
OTU2875 Desulfovibrio Desulfovibrionaceae Proteobacteria
OTU3563 Ruminococcaceae Firmicutes
OTU3652 Acetitomaculum Lachnospiraceae Firmicutes
OTU6078 Ruminococcus Ruminococcaceae Firmicutes
OTU2370 S24-7 Bacteroidetes
OTU4220 Marvinbryantia Lachnospiraceae Firmicutes
OTU3784 Parasutterella Alcaligenaceae Proteobacteria
OTU6059 Ruminococcaceae Firmicutes
OTU1538 Peptococcus Peptococcaceae Firmicutes
OTU441 Bacteroides Bacteroidaceae Bacteroidetes
OTU3157 Lachnospiraceae Firmicutes
OTU4099 Bacteroides Bacteroidaceae Bacteroidetes
OTU2285 Lachnospiraceae Firmicutes
OTU6368 Lachnospiraceae Firmicutes
OTU5073 Bacteroides Bacteroidaceae Bacteroidetes
OTU5622 Bacteroides Bacteroidaceae Bacteroidetes
OTU2417 Proteus Enterobacteriaceae Proteobacteria
OTU5805 Bacteroides Bacteroidaceae Bacteroidetes
OTU2644 Peptococcus Peptococcaceae Firmicutes
OTU5544 Lachnospiraceae Firmicutes
OTU1581 Ruminococcaceae Firmicutes
OTU3697 Odoribacter Porphyromonadaceae Bacteroidetes
OTU953 Ruminococcaceae Firmicutes
OTU3198 S24-7 Bacteroidetes
OTU2801 Lachnospiraceae Firmicutes
OTU6276 Christensenellaceae Firmicutes
OTU2936 Ruminococcaceae Firmicutes
OTU5543 Ruminococcaceae Firmicutes
OTU773 Coprococcus Lachnospiraceae Firmicutes
OTU4801 Anaerotruncus Ruminococcaceae Firmicutes
OTU3892 Tenericutes
OTU5768 Ruminococcaceae Firmicutes
OTU5538 Ruminococcaceae Firmicutes
OTU5746 Ruminococcaceae Firmicutes
OTU376 Christensenella Christensenellaceae Firmicutes
OTU5251 Bilophila Desulfovibrionaceae Proteobacteria
OTU4866 Ruminococcaceae Firmicutes
OTU1990 Candidate_division_TM7
OTU2632 Ruminococcaceae Firmicutes
OTU4629 Ruminococcaceae Firmicutes
OTU5419 Anaerovorax Family_XIII Firmicutes
OTU2249 Ruminococcaceae Firmicutes
OTU544 Desulfovibrio Desulfovibrionaceae Proteobacteria
OTU4794 Desulfovibrionaceae Proteobacteria
OTU5772 Oscillibacter Ruminococcaceae Firmicutes
OTU6065 Butyricimonas Porphyromonadaceae Bacteroidetes
OTU1819 Lachnospiraceae Firmicutes
OTU2641 Helicobacter Helicobacteraceae Proteobacteria

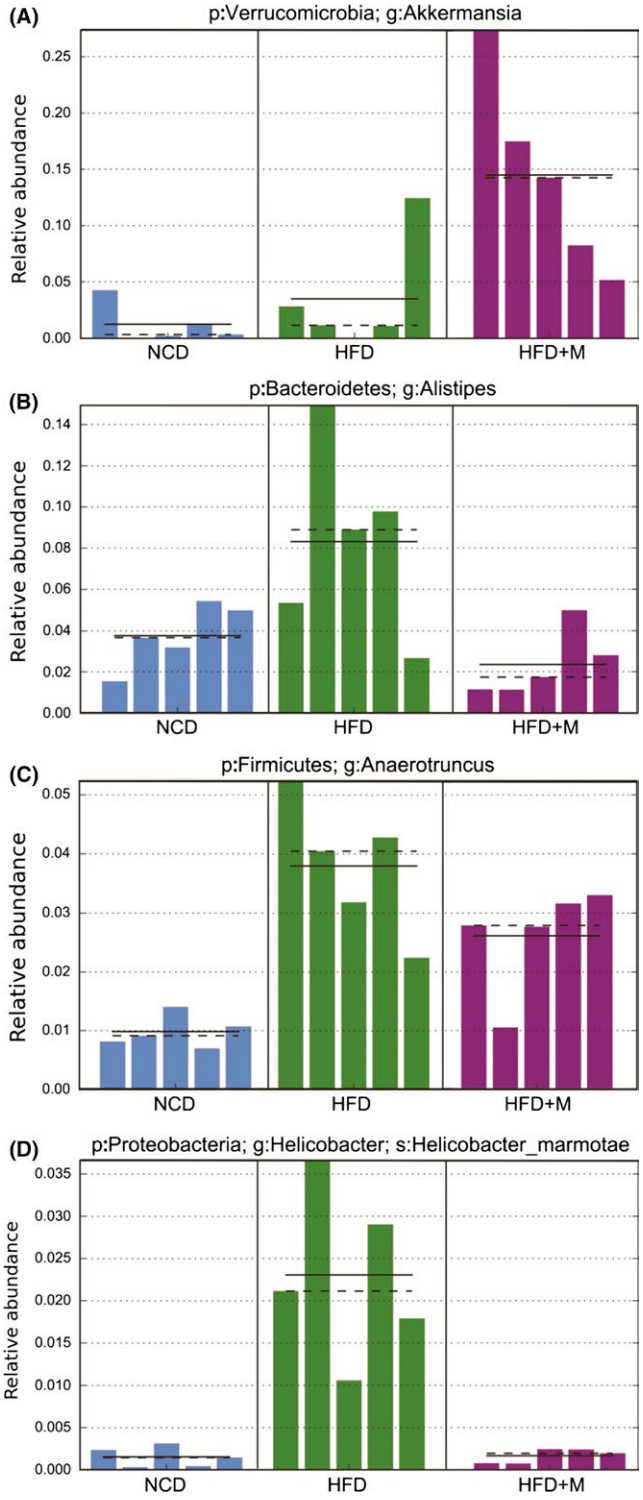

FIGURE 7 The relative abundance of *Akkermansia* (A), *Alistipes* (B), *Anaerotruncus* (C), and *helicobacter marmotae* (D) obtained in fecal microbiota from the LefSe results. Solid and dashed lines indicate mean and median, respectively

melatonin was found to modulate the gut microbiota composition, and the changes induced were associated with obesity.

In our obese mouse model, melatonin treatment significantly reduces body weight gain, fat mass, and epididymal mean adipocyte size to approximately the control levels (Figure 1 and Figure 2A-C). As already mentioned, the gut microbiota of obese humans and rodent models is highly associated with decreased abundances of *Bacteroidetes* and increased abundances of *Firmicutes*.[10,11,45] Our results show that melatonin supplementation significantly increases the abundance of *Bacteroidetes* and decreased the abundance of *Firmicutes* in HFD-fed mice (Figure 5I,J). Growing evidence indicates that the intestinal microbiota plays an important role in modulating host inflammation.[46] In our study, HFD-induced low-grade inflammation can be explained by gut microbiota dysbiosis, which results in increased plasma concentration of LPS. The plasma LPS, also known as endotoxins, are mainly produced by Gram-negative bacteria in the intestinal ecosystem.[47] We observed that the relative abundance of endotoxin-producing bacteria *Desulfovibrionaceae* was decreased in the gut microbiota of HFD+M mice (Figure 6). It was consistent with previous studies showing that the probiotic-enriched diet intervention can reduce the abundance of *Desulfovibrionaceae* in obese individuals.[40] *Akkermansia* is a probiotic, which belongs to the *Verrucomicrobia* phylum and is associated with the nutrition metabolism. Recent studies suggested that *Akkermansia* improves metabolic health and protects from obesity, diabetes, and inflammation in the intestinal tract of rodents.[48-50] Here, melatonin significantly enhanced the level of *Akkermansia* (Figure 5J and Figure 7A). The relative abundances of *Alistipes*[51,52]and *Anaerotruncus*[50] have been correlated with obesity and its associated metabolic disorders in previous studies, and their abundances were also restored by melatonin in HFD-fed mice (Figure 7B-C). Melatonin protects against metabolic dysfunction and oxidative molecular damage in the hepatobiliary and gastrointestinal tract system.[53,54] *Helicobacter marmotae* is considered to be associated with enterohepatic disease.[55] It was reversed by melatonin in HFD-fed mice in the present study (Figure 7D). The aim of this study is to reveal the potential internal connection between gut microbiota and beneficial phenotype with melatonin. The specific mechanism needs further research. Meanwhile, we should note that it is unclear whether melatonin treatment can alter gut microbiota under a normal diet.

Low-grade inflammation is related to NAFLD in human and rodent animals.[36,56] Consistently with a previous study, melatonin alleviated endotoxin-induced NAFLD in mice.[57] In the present study, melatonin treatment significantly reduced HFD-induced hepatic lipid accumulation (Figure 2F,G). The NF-κB signal pathway plays an important role in the development of inflammation, NAFLD, and diabetes.[58] Melatonin decreased the circulating levels of LPS, TNF-α, and IL-6, all markers of systemic low-grade inflammation, and restored the protein expression of NF-κB in liver (Figure 2H-K). Many studies have been reported that melatonin attenuated inflammatory response and oxidative stress by inhibited NFκB activation,[59-61] which was

explored in rat skeletal muscle by increasing IκBα content and decreasing IκBα phosphorylation and IκB kinase α.[62] Additionally, in HFD-fed mice, circulating TG, TC, blood glucose, and insulin levels increased significantly, while the administration of melatonin produced a protective effect and counteracted the increased insulin resistance in obese mice (Figure 3).

Brown adipose tissue (BAT), which expends energy to produce heat, regulates insulin resistance and glucose homeostasis, and promotes a lean and healthy phenotype.[63,64] Several in vivo studies have shown that melatonin treatment regulates the energy metabolism by stimulating BAT and WAT browning.[25,65-67] In the present study, we observed that melatonin administration increases the expression of UCP1 at both the gene and protein levels, enhances fatty acid transport and catabolism, and promotes thermogenesis (Figure 4). Depleting gut microbiota prevents obesity and stimulates the browning of WAT in obese mice.[63] In our model, melatonin decreases the OUT number and reduces the richness and diversity of the gut microbiota, which, to some extent, may support the above hypothesis.

In conclusion, our results show that melatonin treatment modulates the gut microbiota, promoting a decrease in the ratio of *Firmicutes* to *Bacteroidetes* and increasing the relative abundance of *Akkermansia*, while bringing the abundances of *Alistipes*, *Anaerotruncus,* and *Desulfovibrionaceae* back to normal levels, thereby providing beneficial effects against obesity, insulin resistance, liver steatosis, and low-grade inflammation in HFD-fed mice.

ACKNOWLEDGEMENTS

This work was supported by the National Natural Science Foundation of China (NO. 31571164 and NO. 31271207).

CONFLICTS OF INTEREST

The authors have declared that no competing interests exist.

AUTHOR CONTRIBUTIONS

Y.Z. and P.X. contributed to the study design; Y.Z. obtained funding; P.X., J.W., F.H., S.W., and T.X. performed the experiments; P.X., F.H., J.W., X.J., and J.L. analyzed the data; P.X. and Y.Z. wrote the manuscript. All authors reviewed the final manuscript.

REFERENCES

1. World Health Organization. Global Status Report on Noncommunicable Diseases. 2014;79-95.
2. Stevens GA, Singh GM, Lu Y, et al. National, regional, and global trends in adult overweight and obesity prevalences. *Popul Health Metr*. 2012;10:22.
3. Arnold M, Jiang L, Stefanick ML, et al. Duration of adulthood overweight, obesity, and cancer risk in the women's health initiative: a longitudinal study from the united states. *PLoS Med*. 2016;13:e1002081.
4. Jiang Y, Xu Y, Bi YF, et al. Prevalence and trends in overweight and obesity among Chinese adults in 2004-10: data from three nationwide surveys in china. *Lancet*. 2015;386:77.
5. Bhaskaran K, Douglas I, Forbes H, et al. Body-mass index and risk of 22 specific cancers: a population-based cohort study of 5.24 million uk adults. *Lancet*. 2014;384:755-765.
6. Arnold M, Pandeya N, Byrnes G, et al. Global burden of cancer attributable to high body-mass index in 2012: a population-based study. *Lancet Oncol*. 2015;16:36-46.
7. Morgen CS, Sorensen TIA. Obesity global trends in the prevalence of overweight and obesity. *Nat Rev Endocrinol*. 2014;10:513-514.
8. Lim SS, Vos T, Flaxman AD, et al. A comparative risk assessment of burden of disease and injury attributable to 67 risk factors and risk factor clusters in 21 regions, 1990-2010: a systematic analysis for the global burden of disease study 2010. *Lancet*. 2012;380:2224-2260.
9. Turnbaugh PJ, Ley RE, Mahowald MA, et al. An obesity-associated gut microbiome with increased capacity for energy harvest. *Nature*. 2006;444:1027-1031.
10. Ley RE, Backhed F, Turnbaugh P, et al. Obesity alters gut microbial ecology. *Proc Nat Acad Sci USA*. 2005;102:11070-11075.
11. Chang CJ, Lin CS, Lu CC, et al. Ganoderma lucidum reduces obesity in mice by modulating the composition of the gut microbiota. *Nat Commun*. 2015;6:7489.
12. Turnbaugh PJ, Baeckhed F, Fulton L, et al. Diet-induced obesity is linked to marked but reversible alterations in the mouse distal gut microbiome. *Cell Host Microbe*. 2008;3:213-223.
13. Poggeler B, Balzer I, Hardeland R, et al. Pineal hormone melatonin oscillates also in the dinoflagellate gonyaulax-polyedra. *Naturwissenschaften*. 1991;78:268-269.
14. Hardeland R. Melatonin and 5-methoxytryptamine in non-metazoans. *Reprod Nutr Dev*. 1999;39:399-408.
15. Tan DX, Manchester LC, Hardeland R, et al. Melatonin: a hormone, a tissue factor, an autocoid, a paracoid, and an antioxidant vitamin. *J Pineal Res*. 2003;34:75-78.
16. Cipolla-Neto J, Amaral FG, Afeche SC, et al. Melatonin, energy metabolism, and obesity: a review. *J Pineal Res*. 2014;56:371-381.
17. Arnao MB, Hernandez-Ruiz J. Functions of melatonin in plants: a review. *J Pineal Res*. 2015;59:133-150.
18. Prunet-Marcassus B, Desbazeille M, Bros A, et al. Melatonin reduces body weight gain in sprague dawley rats with diet-induced obesity. *Endocrinology*. 2003;144:5347-5352.
19. Rios-Lugo MJ, Cano P, Jimenez-Ortega V, et al. Melatonin effect on plasma adiponectin, leptin, insulin, glucose, triglycerides and cholesterol in normal and high fat-fed rats. *J Pineal Res*. 2010;49:342-348.
20. Agil A, Navarro-Alarcon M, Ruiz R, et al. Beneficial effects of melatonin on obesity and lipid profile in young zucker diabetic fatty rats. *J Pineal Res*. 2011;50:207-212.
21. Nduhirabandi F, Du Toit EF, Blackhurst D, et al. Chronic melatonin consumption prevents obesity-related metabolic abnormalities and protects the heart against myocardial ischemia and reperfusion injury in a prediabetic model of diet-induced obesity. *J Pineal Res*. 2011;50:171-182.
22. Barquilla PC, Pagano ES, Jimenez-Ortega V, et al. Melatonin normalizes clinical and biochemical parameters of mild

inflammation in diet-induced metabolic syndrome in rats. *J Pineal Res*. 2014;57:280-290.
23. Agil A, Reiter RJ, Jimenez-Aranda A, et al. Melatonin ameliorates low-grade inflammation and oxidative stress in young zucker diabetic fatty rats. *J Pineal Res*. 2013;54:381-388.
24. Agil A, Rosado I, Ruiz R, et al. Melatonin improves glucose homeostasis in young zucker diabetic fatty rats. *J Pineal Res*. 2012;52:203-210.
25. Jimenez-Aranda A, Fernandez-Vazquez G, Campos D, et al. Melatonin induces browning of inguinal white adipose tissue in zucker diabetic fatty rats. *J Pineal Res*. 2013;55: 416-423.
26. Agil A, El-Hammadi M, Jimenez-Aranda A, et al. Melatonin reduces hepatic mitochondrial dysfunction in diabetic obese rats. *J Pineal Res*. 2015;59:70-79.
27. Jimenez-Aranda A, Fernandez-Vazquez G, A-Serrano MM, et al. Melatonin improves mitochondrial function in inguinal white adipose tissue of zucker diabetic fatty rats. *J Pineal Res*. 2014;57:103-109
28. Teodoro BG, Baraldi FG, Sampaio IH, et al. Melatonin prevents mitochondrial dysfunction and insulin resistance in rat skeletal muscle. *J Pineal Res*. 2014;57:155-167.
29. Xu PF, Dai S, Wang J, et al. Preventive obesity agent montmorillonite adsorbs dietary lipids and enhances lipid excretion from the digestive tract. *Sci Rep* 2016;6:19659.
30. Xu P, Hong F, Wang J, et al. Microbiome remodeling via the montmorillonite adsorption-excretion axis prevents obesity-related metabolic disorders. *EBioMedicine*. 2017;16:251-261.
31. Xiao L, Wang J, Li J, et al. Ror alpha inhibits adipocyte-conditioned medium-induced colorectal cancer cell proliferation and migration and chick embryo chorioallantoic membrane angiopoiesis. *Am J Phygiol-Cell Phhysiol*. 2015;308: C385-C396.
32. Magoc T, Salzberg SL. Flash: fast length adjustment of short reads to improve genome assemblies. *Bioinformatics*. 2011;27:2957-2963.
33. Edgar RC. Search and clustering orders of magnitude faster than blast. *Bioinformatics*. 2010;26:2460-2461.
34. Caporaso JG, Kuczynski J, Stombaugh J, et al. Qiime allows analysis of high-throughput community sequencing data. *Nat Methods*. 2010;7:335-336.
35. Segata N, Izard J, Waldron L, et al. Metagenomic biomarker discovery and explanation. *Genome Biol*. 2011;12.
36. Harte AL, da Silva NF, Creely SJ, et al. Elevated endotoxin levels in non-alcoholic fatty liver disease. *J Inflamm Lond.* 2010;7:15.
37. Heldmaier G, Hoffmann K. Melatonin stimulates growth of brown adipose-tissue. *Nature*. 1974;247:224-225.
38. Tan DX, Manchester LC, Fuentes-Broto L, et al. Significance and application of melatonin in the regulation of brown adipose tissue metabolism: relation to human obesity. *Obes Rev*. 2011;12:167-188.
39. Kim KA, Gu W, Lee IA, et al. High fat diet-induced gut microbiota exacerbates inflammation and obesity in mice via the tlr4 signaling pathway. *PLoS One*. 2012;7:e47713.
40. Xiao SM, Fei N, Pang XY, et al. A gut microbiota-targeted dietary intervention for amelioration of chronic inflammation underlying metabolic syndrome. *FEMS Microbiol Ecol*. 2014;87: 357-367.
41. Clarke SF, Murphy EF, O'Sullivan O, et al. Targeting the microbiota to address diet-induced obesity: a time dependent challenge. *PLoS One*. 2013;8:e65790.
42. Schulz MD, Atay C, Heringer J, et al. High-fat-diet-mediated dysbiosis promotes intestinal carcinogenesis independently of obesity. *Nature*. 2014;514:508-512.
43. Zanuto R, Siqueira MA, Caperuto LC, et al. Melatonin improves insulin sensitivity independently of weight loss in old obese rats. *J Pineal Res*. 2013;55:156-165.
44. Szewczyk-Golec K, Wozniak A, Reiter RJ. Inter-relationships of the chronobiotic, melatonin, with leptin and adiponectin: implications for obesity. *J Pineal Res*. 2015;59:277-291.
45. Ley RE, Turnbaugh PJ, Klein S, et al. Microbial ecology - human gut microbes associated with obesity. *Nature*. 2006;444:1022-1023.
46. Cani PD, Bibiloni R, Knauf C, et al. Changes in gut microbiota control metabolic endotoxemia-induced inflammation in high-fat diet-induced obesity and diabetes in mice. *Diabetes*. 2008;57:1470-1481.
47. Zhao LP. The gut microbiota and obesity: from correlation to causality. *Nat Rev Microbiol*. 2013;11:639-647.
48. Everard A, Belzer C, Geurts L, et al. Cross-talk between *akkermansia muciniphila* and intestinal epithelium controls diet-induced obesity. *Proc Nat Acad Sci USA*. 2013;110:9066-9071.
49. Caesar R, Tremaroli V, Kovatcheva-Datchary P, et al. Crosstalk between gut microbiota and dietary lipids aggravates wat inflammation through tlr signaling. *Cell Metab*. 2015;22:658-668.
50. Shin NR, Lee JC, Lee HY, et al. An increase in the *akkermansia spp* Population induced by metformin treatment improves glucose homeostasis in diet-induced obese mice. *Gut*. 2014;63:727-735.
51. Zhang CH, Zhang MH, Pang XY, et al. Structural resilience of the gut microbiota in adult mice under high-fat dietary perturbations. *ISME J*. 2012;6:1848-1857.
52. Geurts L, Lazarevic V, Derrien M, et al. Altered gut microbiota and endocannabinoid system tone in obese and diabetic leptin-resistant mice: impact on apelin regulation in adipose tissue. *Front Microbiol*. 2011;2:00149.
53. Brzozowski T, Jaworek J. Basic and clinical aspects of melatonin in the gastrointestinal tract New advancements and future perspectives. *Curr Pharm Design*. 2014;20:4785-4787.
54. Reiter RJ, Rosales-Corral SA, Manchester LC, et al. Melatonin in the biliary tract and liver: health implications. *Curr Pharm Design*. 2014;20:4788-4801.
55. Patterson MM, Rogers AB, Fox JG. Experimental *helicobacter marmotae* infection in a/j mice causes enterohepatic disease. *J Med Microbiol*. 2010;59:1235-1241.
56. Thuy S, Ladurner R, Volynets V, et al. Nonalcoholic fatty liver disease in humans is associated with increased plasma endotoxin and plasminogen activator inhibitor 1 concentrations and with fructose intake. *J Nutr*. 2008;138:1452-1455.
57. Chen X, Zhang C, Zhao M, et al. Melatonin alleviates lipopolysaccharide-induced hepatic srebp-1c activation and lipid accumulation in mice. *J Pineal Res*. 2011;51:416-425.
58. Sajan MP, Nimal S, Pastoor T, et al. Activation of sterol receptor element binding protein-1c and nfkb by atypical protein kinase c in liver mediates lipid abnormalities and insulin resistance in murine obesity models. *Diabetes*. 2008;57:A376-A376.
59. Li Z, Nickkholgh A, Yi X, et al. Melatonin protects kidney grafts from ischemia/reperfusion injury through inhibition of nf-kb and

apoptosis after experimental kidney transplantation. *J Pineal Res*. 2009;46:365-372.
60. Chuffa LG, Fioruci-Fontanelli BA, Mendes LO, et al. Melatonin attenuates the tlr4-mediated inflammatory response through myd88- and trif-dependent signaling pathways in an in vivo model of ovarian cancer. *BMC Cancer*. 2015;15:34.
61. Maldonado MD, Garcia-Moreno H, Gonzalez-Yanes C, et al. Possible involvement of the inhibition of nf-kappab factor in anti-inflammatory actions that melatonin exerts on mast cells. *J Cell Biochem*. 2016;117:1926-1933.
62. Alonso M, Collado PS, Gonzalez-Gallego J. Melatonin inhibits the expression of the inducible isoform of nitric oxide synthase and nuclear factor kappa b activation in rat skeletal muscle. *J Pineal Res*. 2006;41:8-14.
63. Suarez-Zamorano N, Fabbiano S, Chevalier C, et al. Microbiota depletion promotes browning of white adipose tissue and reduces obesity. *Nat Med*. 2015;21:1497-1501.
64. Stanford KI, Middelbeek RJW, Townsend KL, et al. Brown adipose tissue regulates glucose homeostasis and insulin sensitivity. *J Clin Invest*. 2013;123:215-223.
65. Heldmaier G, Steinlechner S, Rafael J, et al. Photoperiodic control and effects of melatonin on nonshivering thermogenesis and brown adipose-tissue. *Science*. 1981;212:917-919.
66. Viswanathan M, Hissa R, George JC. Effects of short photoperiod and melatonin treatment on thermogenesis in the syrian-hamster. *J Pineal Res*. 1986;3:311-321.
67. Holtorf AP, Heldmaier G, Thiele G, et al. Diurnal changes in sensitivity to melatonin in intact and pinealectomized djungarian hamsters - effects on thermogenesis, cold tolerance, and gonads. *J Pineal Res*. 1985;2:393-403.

SUPPORTING INFORMATION

Additional Supporting Information may be found online in the supporting information tab for this article.

How to cite this article: Xu P, Wang J, Hong F, et al. Melatonin prevents obesity through modulation of gut microbiota in mice. *J Pineal Res*. 2017;00:e12399. https://doi.org/10.1111/jpi.12399